Journal of proteome research

Article

pubs.acs.org/jpr

Expression Profile and Regulation of Spore and Parasporal Crystal Formation-Associated Genes in *Bacillus thuringiensis*

Jieping Wang,† Han Mei,† Hongliang Qian, Qing Tang, Xiaocui Liu, Ziniu Yu, and Jin He*

State Key Laboratory of Agricultural Microbiology, College of Life Science and Technology, Huazhong Agricultural University, No. 1 Shizishan Street, Wuhan, Hubei 430070, China

Supporting Information

ABSTRACT: *Bacillus thuringiensis*, a Gram-positive endospore-forming bacterium, is characterized by the formation of parasporal crystals consisting of insecticidal crystal proteins (ICPs) during sporulation. We reveal gene expression profiles and regulatory mechanisms associated with spore and parasporal crystal formation based on transcriptomics and proteomics data of *B. thuringiensis* strain CT-43. During sporulation, five ICP genes encoded by CT-43 were specifically transcribed; moreover, most of the spore structure-, assembly-, and maturation-associated genes were specifically expressed or significantly up-regulated, with significant characteristics of temporal regulation. These findings suggest that it is essential for the cell to maintain efficient operation of transcriptional and translational machinery during sporulation. Our results indicate that the RNA polymerase complex δ and ω subunits, cold shock proteins, sigma factors, and transcriptional factors as well as the E2 subunit of the pyruvate dehydrogenase complex could cooperatively participate in transcriptional regulation via different mechanisms. In particular, differences in processing and modification of ribosomal proteins, rRNA, and tRNA combined with derepression of translational inhibition could boost the rate of ribosome recycling and assembly as well as translation initiation, elongation, and termination efficiency, thereby compensating for the reduction in ribosomal levels. The efficient operation of translational machineries and powerful protein-quality controlling systems would thus ensure biosyntheses of a large quantity of proteins with normal biological functions during sporulation.

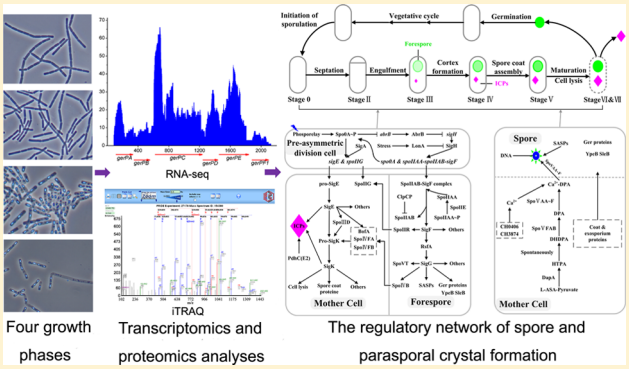

KEYWORDS: *Bacillus thuringiensis, spore and parasporal crystal formation, insecticidal crystal proteins (ICPs), RNA-seq, iTRAQ, LC−MS/MS, gene expression profiles, transcriptional regulation, translational regulation, metabolic regulation*

INTRODUCTION

During sporulation, the Gram-positive entomopathogenic bacterium *Bacillus thuringiensis* forms parasporal crystals consisting of insecticidal crystal proteins (ICPs), which typically represent up to 25% of the cell dry mass of the sporulated cells.[1] The spectrum of ICP insecticidal activity includes 12 orders of insect (including Lepidoptera, Diptera, and Coleoptera), nematode, and even human cancer cells.[2,3] Importantly, *B. thuringiensis* is one of the safest microbial products known.[4] With these unique advantages, *B. thuringiensis* has been used worldwide for many years as an environmentally compatible biopesticide to control insects that affect agriculture and public health.

The complete 6.15 Mb genome of *B. thuringiensis* CT-43 has been sequenced by our laboratory;[5] it contains 11 replicons, a circular chromosome encoding 5529 open reading frames (ORFs), and 10 circular plasmids totally encoding 737 ORFs. The number of ORFs encoded by the CT-43 chromosome is obviously higher than the 4.21 Mb *Bacillus subtilis* 168 genome, which comprises only 4100 ORFs.[6] From an evolutionary perspective, CT-43 obtained some unique gene families, such as *cry* genes, by horizontal gene transfer. Moreover, the expansion of several gene families by gene duplication in CT-43 is greater than that of *B. subtilis* 168. For example, the largest family in *B. subtilis* 168 contains 77 putative ATP-binding transport proteins,[6] while CT-43 encodes at least 101 members of this gene family. In addition, the CT-43 chromosome encodes 312 transcriptional factors (TFs) and 103 members of two-component systems (TCSs), whereas the *B. subtilis* 168 chromosome encodes 237 TFs and 70 TCSs, respectively.[7,8] This evidence implies that *B. thuringiensis* involves a more complicated regulation network of gene expression and can adapt to a wider range of environmental fluctuations.[7]

High-throughput transcriptomic and quantitative proteomic analyses of the four different growth phases of CT-43 were comprehensively evaluated using the Illumina high-throughput sequencing (RNA-seq) method and isobaric tags for relative and absolute quantitation (iTRAQ) technique combined with liquid chromatography−mass spectrometry/mass spectrometry (LC−MS/MS), respectively. In RNA-seq data, the total number

Received: April 22, 2013
Published: November 12, 2013

of clean-reads for the four growth phases were 926 755, 1 096 665, 577 810, and 1 493 721, respectively, with an average length of 110 nt. Therefore, the sequencing coverage of each sample reached 10- to 27-fold. In iTRAQ data, a total of 1756 proteins were identified in eight samples (two biological replicates were included for each growth phase), representing ~28% of the total 6266 proteins encoded by CT-43 genome.[9] The results allowed elucidation of the regulatory mechanisms underlying the metabolic pathways and energy supply associated with sporulation and parasporal crystal formation in *B. thuringiensis*.[9] Here we focused on the gene expression profiles and regulatory mechanisms involved in spore and parasporal crystal formation in *B. thuringiensis*.

MATERIALS AND METHODS

RNA-seq and iTRAQ Analyses

Bacterial cultivation, cDNA library construction, RNA-seq, iTRAQ, LC−MS/MS, bioinformatics, and statistical analyses were carried out as previously described.[9] In brief, two biological replicate cell samples of the *B. thuringiensis* strain CT-43 were collected at 7, 9, 13, and 22 h. Each sample was divided into two parts for whole-genome transcriptomics and proteomics analyses. For RNA-seq, total RNA was extracted from each sample and treated with terminator 5′-phosphate-dependent exonuclease (Epicenter, Madison, WI) to deplete processed RNAs.[10] Double-stranded cDNA libraries were constructed and sequenced with an Illumina Genome Analyzer IIx. The reads of each sample were mapped to the CT-43 genome using BlastN with a threshold *e* value of 0.00001 and the "-F F" parameter.[11] The expression level of each gene was reported as reads per kilobase of coding sequence per million mapped reads (RPKM), and differentially expressed genes were identified by the DEGseq package.[12] We used FDR $\leq$ 0.001 and an absolute value of $\log_2$ ratio $\geq$1 as the threshold to judge the significance of gene expression difference.

For iTRAQ-LC−MS/MS, total proteins were extracted from each sample and tryptically digested. The resulted peptides were labeled individually with 8-plex iTRAQ reagents (Applied Biosystems, Foster City, CA) at room temperature for 2 h as follows: 7 h-1, 113; 7 h-2, 114; 9 h-1, 115; 9 h-2, 116; 13 h-1, 117; 13 h-2, 118; 22 h-1, 119; and 22 h-2, 121. The labeled samples were pooled and then resolved into 12 fractions using an Ultremex SCX column (Phenomenex, Torrance, CA). After desalting using a Strata X C18 column (Phenomenex) and drying under vacuum, the labeled samples were subjected to LC−MS/MS analysis using a splitless nanoACQuity (Waters, Milford, MA) system coupled to a Triple TOF 5600 system (AB SCIEX, Concord, ON). Spectra from the 12 fractions were combined into one MGF (Mascot generic format) file and searched against the *B. thuringiensis* CT-43 protein database (6266 sequences, including 5529 proteins of the chromosome and 737 proteins of the plasmids) combined with the reversed version of all protein sequences using the Mascot search engine (2.3.02 version, Matrix Science). In the final search results, the false discovery rate (FDR) was <1.5%. The iTRAQ 8-plex was chosen for quantification during the search. A protein with $\geq$1.5-fold difference in the expression level and a *p* value $\leq$0.05 was regarded as being differentially expressed in our data.[13,14]

The iTRAQ labeling, SCX fractionation, LC−MS/MS analysis processes, and associated search parameters are also detailedly described in the Supporting Information.

Determination of Expression of ICP Genes at the Protein Level

Strain CT-43 was grown under the same conditions as above. At each time point (7, 9, 11, 13, 15, 17, 19, 21, 22, and 23 h), 20 mL of cultures was separately collected and centrifuged for 15 min (6000*g*, 4 °C). Each cell pellet was then separately resuspended in phosphate-buffered saline (137 mM NaCl, 2.7 mM KCl, 10.1 mM Na_2HPO_4, 1.8 mM KH_2PO_4, pH 7.4); then, the suspension was sonicated on ice for 30 min (alternating 15 s sonication and 10 s pause at 130 W) using an ultrasonic processor model VC-130 (Sonics and Materials, Newtown, CT), and centrifuged for 10 min (12 000*g*, 4 °C). Each precipitate (cellular debris) was separately washed with 1 mol/L of NaCl and sterile water. After that, the washed precipitate was resuspended in 500 μL of 50 mmol/L Na_2CO_3−$NaHCO_3$ (pH 10.0) containing 5% β-mercaptoethanol and incubated at 37 °C for 1 h to dissolve the parasporal crystals. Thereafter, the samples were centrifuged for 10 min (12 000*g*, 4 °C), and the supernatants were analyzed by SDS-PAGE.

MS Identification of Proteins from ICP Bands

Two ICP bands corresponding to the 71 and 140 kDa were excised from SDS-PAGE gel (named as Cry_sample_1 and Cry_sample_2, respectively; see Supplementary Figure S1 in the Supporting Information). They were subjected to in-gel reduction, alkylation, and digestion with trypsin as follows: samples were dehydrated with 500 μL of ACN, incubated for 60 min at 56 °C with 200 μL of 10 mM DTT in 25 mM ammonium bicarbonate buffer and then incubated for 45 min at room temperature in darkness with 200 μL of 55 mM iodoacetamide in 25 mM $(NH_4)HCO_3$ buffer. They were then washed twice with 25 mM $(NH_4)HCO_3$ buffer and dehydrated with 500 μL of ACN, proteolyzed by trypsin overnight at 37 °C, and subsequently treated with 5% FA to stop proteolysis.

The peptides were then eluted from the gel pieces once with 200 μL of 50% ACN and 0.1% FA and twice with 200 μL of 100% ACN and 0.1% FA. The eluted fractions were collected and dried under vacuum. Each fraction was resuspended in certain volume of buffer A (2% ACN, 0.1% FA) and centrifuged at 20 000*g* for 10 min. The final concentration of the peptide in each fraction was ~0.5 μg/μL on average. Using an autosampler, 10 μL of supernatant was loaded on a 2 cm C18 trap column (inner diameter 200 μm) on a Shimadzu LC-20AD nanoHPLC. Peptides were eluted onto a resolving 10 cm analytical C18 column (inner diameter 75 μm) that was assembled in-house. The samples were loaded at 15 μL/min for 4 min and eluted with a 44 min gradient at 400 nL/min from 2 to 35% B (98% ACN, 0.1% FA), followed by a 2 min linear gradient to 80% B, maintenance at 80% B for 4 min, and finally a return to 2% B in 1 min.

The MS identification process and search parameters were the same as the iTRAQ experiments, which are described in detail in the Supporting Information.

Accession Number

The RNA-seq data from this article are available as raw short reads data in the NCBI's GEO database under accession number GSE39479. Mass spectrometry data of the iTRAQ experiment from this article are deposited in the mzML format in the ProteomeExchange database (http://proteomexchange.org/) under accession number PXD000020 through the PRIDE Web site (http://www.ebi.ac.uk/pride/). Additionally, the MS data of the two ICP bands have been deposited to the ProteomeXchange with identifier PXD000425.

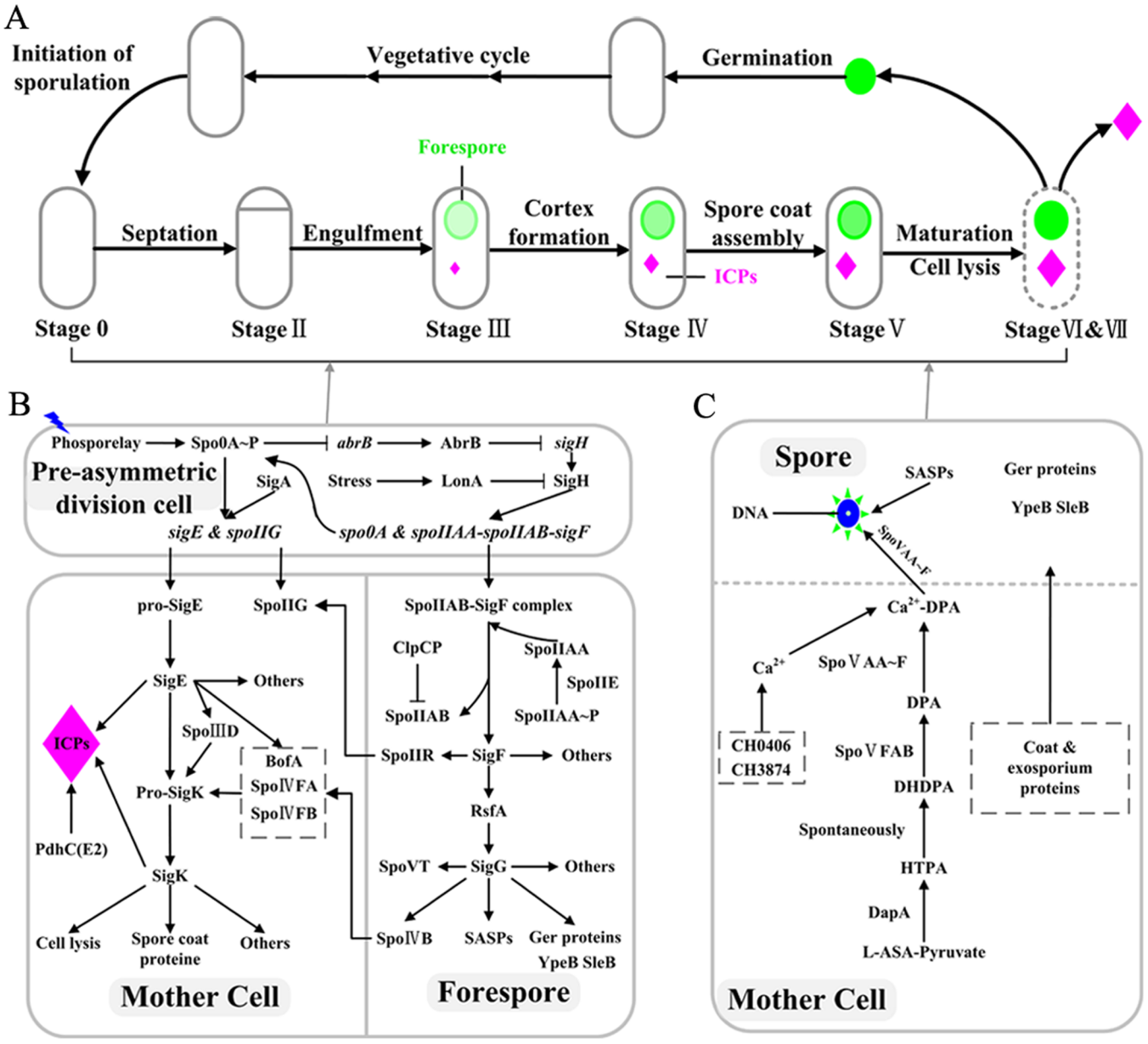

Figure 1. Spore and parasporal crystal formation and the regulatory network of gene expression in *B. thuringiensis*. (A) Life cycle of *B. thurigiensis* and the formation processes of spore and parasporal crystal. The spore and parasporal crystal are emphasized by green and purple colors, respectively. (B) Temporal and spatial regulation network of σ factors and transcriptional factors. This part is drawn mainly according to figure 2 in ref 64. (C) Biosyntheses and transport of spore structural components.

RESULTS AND DISCUSSION

Process of Spore Formation in *B. thuringiensis*

Sporulation in *B. thuringiensis* is characterized by seven stages: stages 0 to I, axial filament formation; stage II, forespore septum formation and asymmetric cell division; stage III, engulfment, forespore formation, and the first appearance of parasporal crystals; stages IV to VI, cortex, coat, and exosporium assembly and development of parasporal crystals; and stage VII, spore maturation and mother cell lysis and spore and parasporal crystal release[9,15−17] (Figure 1A).

Among the four time points selected,[9] 7 h (midlog growth phase) represented vegetative growth stage, 9 h (early stationary growth phase) might cover stages 0 to II, 13 h (midstationary growth phase, the proportion of sporulating cells reached about 30%) might include stages IV to VI, and 22 h (spore maturation and mother cell lysis phase) mainly represented stages VI and VII, owing to sporulating population heterogeneity.[18]

ICP Gene Expression Profiles

In CT-43, the largest plasmid pCT281 (281.14 kb) encodes four ICP genes, *cry1Aa3*, *cry1Ia14*, *cry2Aa9*, and *cry2Ab1*, and the second largest plasmid pCT127 (127.86 kb) contains another ICP gene, *cry1Ba1*. The results of RNA-seq indicated that the transcripts of these genes were all specifically detected from 13 h (Table 1). Unfortunately, the ICPs were not detected at all by iTRAQ possibly because the ICPs are wrapped in compact parasporal crystals upon production and the protein sample preparation procedure did not include an alkali dissolution step (e.g., treatment with Na_2CO_3−$NaHCO_3$, pH 10.0 for 1 h at 37 °C), which is necessary to dissolve ICPs out of the parasporal crystals. However, the parasporal crystals composed of ICPs

dx.doi.org/10.1021/pr4003728 | J. Proteome Res. 2013, 12, 5487−5501

Table 1. Transcriptional Level of the Genes Encoding ICPs and an Accessory Protein

gene name	gene code	molecular weight (kDa)	RPKM			
			7 h	9 h	13 h	22 h
cry2Ab1	pCT281.272	71	0	0	96	8
cry1Aa3	pCT281.277	133	0	0	6362	479
cry1Ia14	pCT281.278	81	0	0	162	0
cry2Aa9	pCT281.286	71	0	0	7553	43
ORF2	pCT281.287	29	0	0	20231	17
cry1Ba1	pCT127.021	140	0	0	26134	6853

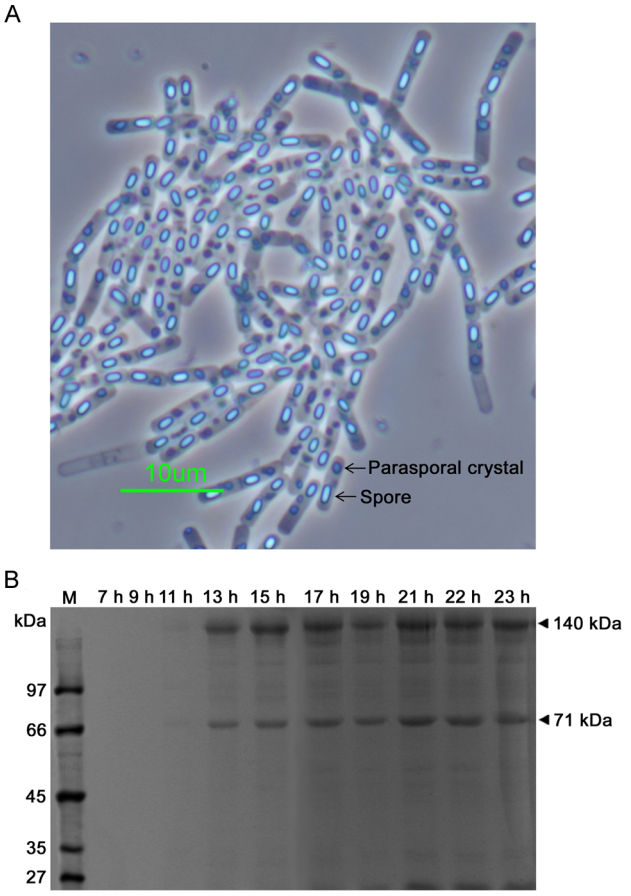

Figure 2. Expression of ICP genes at the protein level. (A) Presence of parasporal crystals determined by phase-contrast microscopy. *B. thuringiensis* strain CT-43 was grown in GYS medium for 17 h at 28 °C and 200 rpm, which allowed sporulation process to occur. Then, the sample was observed under a phase-contrast microscopy (Nikon ECLIPSE E6000, Nikon, Tokyo, Japan). The scale bar represents 10 μm. (B) Time course of the ICPs production in *B. thuringiensis* strain CT-43.

could be clearly observed in the cells during sporulation under a phase-contrast microscope (Figure 2A), and through the alkali dissolution step, two prominent ICP bands could be acquired, as shown in Figure 2B.

According to the RPKM value of each gene, the transcriptional levels of the genes *cry1Ba1*, *cry2Aa9*, and *cry1Aa3* were higher than others, suggesting that the proteins Cry1Ba1, Cry2Aa9, and Cry1Aa3 might be the main components of parasporal crystals in CT-43. By performing an additional MS identification (Supplementary Table S1 in the Supporting Information), we confirmed that the 140 kDa band (the main band) shown in Figure 2B was composed of Cry1Ba1 and Cry1Aa3, while the 71 kDa band (the second band) was Cry2Aa9 and Cry2Ab1, together with the degraded parts of Cry1Ba1 and Cry1Aa3. According to the numbers of unique peptides identified, Cry1Ba1 (the main component of the main band), Cry2Aa9 (the main component of the second band), and Cry1Aa3 (the second component of the main band) were high-abundant proteins. The result was in accordance with the transcriptome data. The mode of parasporal crystal assembly likely varies with the ICP type. The larger-sized ICPs (~130 kDa) seem to form parasporal crystals by self-assembly, while the smaller-sized ICPs (71 kDa or less) that consist only of an insecticidal N-terminal region require accessory proteins (such as P20 and ORF2) for parasporal crystal assembly.[19,20] The ORF2 (29 kDa) in the same operon that contains the *cry2Aa9* gene was also expressed at very high levels (Table 1), so it would act as an accessory protein to facilitate Cry2Aa9 assembling into parasporal crystals.[20]

Expression Profiles of the Spore Structure and Assembly Associated Genes

The spore structure and chemical composition play major roles in spore resistance. From exterior to interior, the concentrically arranged layers of *B. thuringiensis* spores include the exosporium, coat, outer membrane, cortex, germ cell wall, inner membrane, and central core.[21,22] Next, the expression profiles of the spore structure, assembly, and maturation-associated genes were partially and briefly analyzed in the order from interior to exterior.

Core. The core is the innermost layer of the spore and contains DNA, ribosomes, tRNA, and many enzymes. The most significant differences between the growing cell cytoplasm and the core are: (i) a large decrease in core water content (only 25−50% of core wet weight), (ii) high levels of dipicolinic acid (DPA) (5−15% of core dry weight), and (iii) the saturation of DNA with α/β-type small, acid-soluble spore proteins (SASPs).[21,22]

DPA was confirmed to be extremely important in spore resistance and stability, which is a major driving force for the spore to accumulate such high levels of this small molecule.[23] DPA is produced via a branch off of the lysine biosynthetic pathway. One step in this pathway is the condensation of aspartate semialdehyde and pyruvate to produce dihydrodipicolinic acid (DHDPA) catalyzed by DapA (dihydrodipicolinate synthase).[24] In the last step, DHDPA is oxidized into DPA by the enzymes SpoVFA and SpoVFB, the products of the *spoVFAB* operon[25] (Figure 1C). Our RNA-seq results showed that the *dapA2* gene was highly expressed at 7 and 9 h and obviously down-regulated at 13 h, whereas the mRNA of another isozyme gene *dapA1* was detected only at low levels at 13 h (Supplementary Table S2 and Figure S2 in the Supporting Information). At the protein level, DapA2 was identified, and its abundance showed no increase at 13 h, which leads to the question of whether DHDPA was produced during the exponential growth phase. The increase at both the mRNA and protein levels

dx.doi.org/10.1021/pr4003728 | J. Proteome Res. 2013, 12, 5487−5501

Table 2. Transcriptional Profiles of the Spore Peptidoglycan Synthesis-Associated Genes in *B. thuringiensis* CT-43

gene	gene code	function	RPKM			
			7 h	9 h	13 h	22 h
murA1	CH5327	UDP-*N*-acetylglucosamine 1-carboxyvinyltransferase	175	253	1153	918
murA2	CH5374	UDP-*N*-acetylglucosamine 1-carboxyvinyltransferase	455	304	244	0
murB	CH3910	UDP-*N*-acetylenolpyruvoylglucosamine reductase	1579	2835	146	0
murB2	CH5132	UDP-*N*-acetylenolpyruvoylglucosamine reductase	16	24	49	7
murC	CH4710	UDP-*N*-acetylmuramate-L-alanine ligase	102	162	187	58
murD	CH3913	UDP-*N*-acetylmuramoyl-L-alanyl-D-glutamate synthetase	102	63	162	74
murE	CH3915	UDP-*N*-acetylmuramoylalanyl-D-glutamate- 2,6-diaminopimelate ligase	70	172	130	0
murF	CH0220	UDP-*N*-acetylmuramoylalanyl-D-glutamyl	122	75	89	23
murF	CH2116	2,6-diaminopimelate-D-alanyl-D-alanyl ligase	4	7	33	14
murG	CH3690	*N*-acetylglucosaminyl transferase	0	0	107	0
murG	CH3911	*N*-acetylglucosaminyl transferase	0	0	158	0
murG2	CH4267	*N*-acetylglucosaminyl transferase	91	152	97	56
murG2	CH4269	*N*-acetylglucosaminyl transferase	74	235	23	23
mraY	CH3914	phospho-*N*-acetylmuramoyl-pentapeptide-transferase	54	29	118	58
bacA1	CH0658	undecaprenyl pyrophosphate phosphatase	4	8	28	23
bacA2	CH1313	undecaprenyl pyrophosphate phosphatase	371	145	269	0
bacB	CH2689	undecaprenyl pyrophosphate phosphatase	0	0	478	20
	CH1513	oligosaccharide translocase (flippase)	0	0	261	0
	CH5470	oligosaccharide translocase (flippase)	40	5	67	0
dacA	CH0009	D-alanyl-D-alanine carboxypeptidase (low MW PBP5)	90	45	232	0
dacB	CH1296	muramoyltetrapeptide carboxypeptidase (low MW PBP5*)	123	129	1314	14
	CH1207	D-alanyl-D-alanine carboxypeptidase	21	10	26	0
dacB	CH1397	D-alanyl-D-alanine carboxypeptidase (low MW PBP5*)	0	0	333	0
spmA	CH1398	spore maturation protein A	0	0	218	0
spmB	CH1399	spore maturation protein B	0	0	833	0
	CH1490	thermostable carboxypeptidase 1	669	251	98	20
	CH1620	D-alanyl-D-alanine carboxypeptidase	8	48	137	0
	CH1903	D-alanyl-D-alanine carboxypeptidase	9	36	18	0
	CH2011	D-alanyl-D-alanine carboxypeptidase	89	91	204	89
	CH2482	D-alanyl-D-alanine carboxypeptidase	0	0	50	0
	CH3010	D-alanyl-D-alanine carboxypeptidase	8	41	58	12
	CH3218	D-alanyl-D-alanine carboxypeptidase	74	296	141	0
	CH3463	D-alanyl-D-alanine carboxypeptidase	0	0	694	0
	CH3494	D-alanyl-D-alanine carboxypeptidase	29	213	174	0
dacF	CH4083	D-alanyl-D-alanine carboxypeptidase (low MW PBP)	0	0	2135	0
	CH5069	D-alanyl-D-alanine carboxypeptidase	0	0	126	0
	CH5429	D-alanyl-D-alanine carboxypeptidase	7	5	36	4
	CH0425	penicillin-binding protein	0	0	112	0
pbpF	CH1020	penicillin-binding protein (class A PBP)	0	0	123	0
	CH1383	penicillin-binding protein	0	0	256	0
	CH1476	penicillin-binding protein	0	28	45	0
	CH1616	penicillin-binding protein	0	42	84	43
	CH2155	penicillin-binding protein	62	132	174	0
	CH2245	penicillin-binding protein	51	47	166	0
	CH2619	penicillin-binding protein	0	53	0	0
	CH2644	penicillin-binding protein	47	0	0	0
	CH2668	penicillin-binding protein	0	0	234	0
	CH3054	penicillin-binding protein	60	106	77	7
	CH3426	penicillin-binding protein	0	88	101	13
	CH4049	penicillin-binding protein	137	200	386	0
	CH4289	penicillin-binding protein	151	215	81	0
ywhE	CH4395	penicillin-binding protein (class A PBP)	0	0	3291	0
	CH5415	penicillin-binding protein	0	0	271	0
cwlD	CH0144	spore-specific *N*-acetylmuramoyl-L-alanine amidase	0	0	262	0
cwlD2	CH1421	*N*-acetylmuramoyl-L-alanine amidase	0	0	750	0
pdaA?	CH0306	polysaccharide deacetylase	14	3	31	14
padA	CH0411	*N*-acetylmuramic acid deacetylase	11	30	35	0
cwlC	CH2172	spore-specific *N*-acetylmuramoyl-L-alanine amidase	0	0	89	20135
cwlB	CH2234	*N*-acetylmuramoyl-L-alanine amidase	12	22	23	7494

dx.doi.org/10.1021/pr4003728 | *J. Proteome Res.* 2013, 12, 5487−5501

Table 2. continued

gene	gene code	function	RPKM 7 h	9 h	13 h	22 h
cwlH	CH2815	*N*-acetylmuramoyl-L-alanine amidase	0	0	39	1246
cwlH2	CH3622	*N*-acetylmuramoyl-L-alanine amidase	0	0	0	1652
spoVB	CH4429	stage V sporulation protein B	0	0	134	0
spoVD	CH3916	sporulation specific D,D-transpeptidase (class B PBP)	92	227	489	0
spoVE	CH3912	stage V sporulation protein E	87	313	539	0
spoVR	CH0741	stage V sporulation protein R	0	0	1947	0
spoVK	CH3647	cell division protein FtsH	0	0	1198	38
spoVS	CH2092	stage V sporulation protein S	803	2428	2147	7596
spoVS2	CH3719	stage V sporulation protein S	4622	6601	4720	0
spoVT	CH0049	stage V sporulation protein T	524	363	674	116
	CH1407	cell wall endopeptidase	0	0	599	0
ftsW	CH0984	cell division protein FtsW	38	20	18	0
ftsW	CH1140	cell division protein FtsW	0	0	23	0
ftsW	CH3954	cell division protein FtsW	283	163	80	0
rodA	CH4172	rod shape-determining protein RodA	121	169	119	0

of the enzymes SpoVFA and SpoVFB during sporulation suggests that DPA synthesis is temporally activated (Supplementary Table S2 in the Supporting Information). Meanwhile, Cax (calcium/proton antiporter) and a calcium-transporting ATPase (CH3874) were also up-regulated at both the mRNA and protein levels during sporulation, which possibly satisfies the need of DPA to form a 1:1 chelate with Ca^{2+}. DPA is synthesized only in the mother cell compartment of the sporulating cell and is ultimately located only in the core of the spore (Figure 1C). The 1:1 chelate of DPA and Ca^{2+} is taken up into the forespore via proteins encoded by the *spoVAA*∼*F* operon[26] (Figure 1C), which was revealed by RNA-seq to be specifically induced (throughout the manuscript, "specially induced" at a time point indicates that the gene/protein is not transcribed/expressed before this time point) at 13 h at relatively low levels (Supplementary Table S2 in the Supporting Information).

The α/β-type SASPs are extremely abundant in the spore core, comprising 3−6% of total spore protein.[22] Moreover, they are synthesized only in the developing forespore during sporulation.[22] They can saturate the spore DNA and alter its structure, contributing to the resistance of the spores to heat, UV radiation, and many chemicals.[21] The CT-43 chromosome contains 12 genes encoding the SASPs, and the mRNAs of these genes could be detected only after 13 h (Supplementary Table S2 and Figure S2 in the Supporting Information). Among the eight SASPs identified by iTRAQ, (i) CH0446, SspN and SspB seemed to be produced starting at 9 h according to the extremely large difference times at 7 h versus 9 h; (ii) the abundance of six SASPs was significantly increased at 13 h compared with 9 h, including SspK (5.6-fold), SasP1 (10.7-fold), CH1242 (7.3-fold), CH1940 (5.4-fold), SasP2 (4.8-fold), and SspB (11.3-fold); and (iii) the abundance of these SASPs all remained almost unchanged at 22 h compared with 13 h (Supplementary Table S2 in the Supporting Information). Thus, these results demonstrate the temporal nature of the SASP biosynthesis in the forespore.[22]

Cortex. After engulfment, the forespore becomes a double-membrane-bound cell within the mother cell. Two layers of spore peptidoglycan (PG) are synthesized within the space between the inner and outer membranes.[27] The inner layer of spore PG, the germ cell wall, is synthesized first, followed by the outer layer, the cortex.[27] The PG of the germ cell wall synthesized within the forespore has a structure that is probably identical to that of vegetative cells, while the cortex PG synthesized within the mother cell has several structural modifications relative to vegetative cell PG.[21] In *B. subtilis*, the cortex PG differs from the vegetative cell PG most dramatically in: (i) the absence of teichoic acids; (ii) the removal of many peptide side chains, ∼1/4 of the *N*-acetyl muramic acid (NAM) residues carrying a single L-alanine residue; and (iii) conversion of ∼50% of the NAM residues to muramic-δ-lactam, an important marker of the cortex PG.[21,27,28]

In bacteria, cytoplasmic PG precursors are synthesized as the UDP-linked *N*-acetyl glucosamine (NAG) and NAM. Amino acids are sequentially added to UDP-NAM to produce the pentapeptide side chain. The NAM-pentapeptide is then transferred to an undecaprenol lipid carrier to produce Lipid I, with subsequent addition of NAG from UDP-NAG to produce Lipid II. All of these cytoplasmic steps are catalyzed by the *mur* gene products (MurA∼G plus MraY).[28] Subsequently, Lipid II is flipped across the membrane into the intermembrane space by flippases, which include two protein families: the COG2244 family including SpoVB and MurJ[29] as well as the SEDS family of integral membrane proteins, which includes FtsW, RodA, and SpoVE. The disaccharide−pentapeptide subunits are polymerized into glycan strands, and the peptide side chains are utilized to cross-link the strands into a network via the glycosyl transferase and transpeptidase activities carried jointly by penicillin-binding proteins (PBPs).[28,29]

Our results demonstrated that most enzymes required for vegetative cell PG synthesis remained essentially constant at both the mRNA and protein levels during sporulation (Table 2, Supplementary Table S3 and Figure S3 in the Supporting Information), suggesting that some enzymes required for spore PG synthesis are certainly shared with vegetative cell PG synthesis machinery.[28] Many enzymes were significantly up-regulated or specifically induced during sporulation (Table 2, Supplementary Table S3 and Figure S3 in the Supporting Information), indicating that these enzymes could be specific for spore PG synthesis and modification.

At the mRNA level, some *mur* genes were obviously up-regulated at 13 h compared with 7 h (unless otherwise noted, "7 h" is hereafter used as the comparative object), including *murA1* (more than six-fold), *murB2* (about three-fold), *murE* (about two-fold), *murF* CH2116 (about eight-fold), and *mraY* (about two-fold). In addition, two *murG* genes, CH3690 and CH3911, were specifically induced at 13 h. At the protein level,

dx.doi.org/10.1021/pr4003728 | J. Proteome Res. 2013, 12, 5487−5501

eight enzymes (including MurA1, MurA2, MurB2, MurC, MurD, MurE, MurF CH0220, and MurG CH3911) were identified by iTRAQ, and the abundance of seven enzymes remained almost unchanged, except MurA1, which was down-regulated by 1.6-, 2.5-, and 1.7-fold at 9, 13, and 22 h, respectively (Supplementary Table S3 in the Supporting Information).

Among the significant functionally redundant PBPs and flippases, some enzymes have been confirmed to participate in cortex PG synthesis, including: Class A PBPs, PbpF and YwhE; Class B PBPs, SpoVD and SpoVE; low-MW PBPs, DacA, DacB, and DacF, as well as SpoVB.[28,29] Our RNA-seq data showed that 17 genes of these functional groups were specifically induced during sporulation, which included the *dacB-spmA-spmB* operon, *dacF*, *pbpF*, *spoVB*, and *ywhE*. In addition, 14 genes were up-regulated at 13 h by 2- to 21-fold, including *dacA* (2-fold), *dacB* (10-fold), CH1620 (17-fold), CH3218 (21-fold), *spoVD* (5-fold), and *spoVE* (6-fold) (Table 2). In iTRAQ data, nine enzymes of these functional groups were identified. DacF, CH2155, CH2245, and CH4289 were up-regulated by 1.6-, 3.6-, 1.2-, and 1.6-fold at 9 h and by 2.1-, 2.2-, 1.5-, and 1.3-fold at 13 h, respectively; DacA, CH1476, and CH1490 remained unchanged, while two DacB proteins, CH1296 and CH1397, could not be quantified (Supplementary Table S3 in the Supporting Information).

During muramic-δ-lactam formation, the *N*-acetylmuramoyl-L-alanine amidase encoded by *cwlD*, removes a peptide side chain from the NAM residue, and the *N*-acetylmuramic acid deacetylase, encoded by *pdaA*, sequentially catalyzes the deacetylation of muramic acid and lactam ring formation.[30,31] At the mRNA level, two *cwlD* genes, CH0144 and CH1421, were specifically induced, and two *pdaA* genes, CH0306 and CH0411, were both up-regulated by about three-fold at 13 h (Table 2). In iTRAQ data, the abundance of CwlD2 (CH1421) was increased by two-fold at 13 h and eight-fold at 22 h; the two PdaA enzymes were identified but failed to be quantified (Supplementary Table S3 in the Supporting Information). In addition, additional four *N*-acetylmuramoyl-L-alanine amidase genes (*cwlC*, *cwlB*, *cwlH*, and *cwlH2*) were highly expressed at the mRNA level only at 22 h, implying that these enzymes participate in mother cell lysis or cortex hydrolysis during spore germination.[21]

Coat and Exosporium. In *B. subtilis*, the coat is the outermost layer of the spore and is composed of three layers: the inner coat, the outer coat, and the crust.[32,33] In the *Bacillus cereus* group, which includes *Bacillus anthracis*, *B. cereus*, and *B. thuringiensis*, the coat contains only two layers: the inner coat and outer coat, but the outermost layer consists of a different type called the exosporium.[33,34] The function, structure, and assembly of the coat and exosporium have been comprehensively and systematically discussed in many excellent reviews.[21,22,33,34] On the basis of our RNA-seq and iTRAQ data from CT-43, we focused on the expression profiles of the coat and exosporium structure-, assembly-, and maturation-associated genes at both the mRNA and protein levels.

In RNA-seq data, the transcripts of the overwhelming majority of the coat and exosporium-associated genes were specifically detected at a very high abundance at 13 or 22 h (Table 3 and Supplementary Figure S4 in the Supporting Information). However, most of the 35 proteins identified by iTRAQ could be detected from 7 h, except that a few proteins (including BxpB, CotJB, CotY, CwlJ, ExsY, SpoIVA, SpoVID, and YpzA) seemed to be specifically expressed during sporulation, according to the extremely large differences in protein abundance (Table 4). These results demonstrate that many coat and exosporium-associated proteins are not synthesized de novo during sporulation but rather are packaged from preexisting stocks.[35,36] The highest mRNA levels of many genes appeared at 13 h, while the protein abundances of these genes reached maximum values at 22 h, obviously displaying a temporal delay in protein expression relative to mRNA expression (Tables 3 and 4). In addition, the mRNAs of many genes could not be detected in both the 7 and 9 h samples, but the proteins encoded by these genes were detectable in the samples (Tables 3 and 4). Some studies in other species also found that the mRNA and protein changes of many genes were not correlated,[37−39] which could be due to differential regulation of mRNA and protein expression, stability, and degradation.[37]

The total number of coat proteins is estimated to be more than 70 in *B. subtilis*, and at least 50 coat proteins and morphogenetic factors are encoded in the genomes of the *B. cereus* group[34,40] (Table 3). The morphogenetic factors SpoIVA, SpoVID, ExsA/SafA, and CotE that are conserved in the genus *Bacillus* play major roles in coat morphogenesis.[31,34] In *B. subtilis*, SpoIVA is located in close proximity to the forespore outer membrane and acts as the site of coat attachment, while SafA and CotE are necessary for the assembly of the inner coat and outer coat, respectively.[32−34] Our proteomics data showed that the abundances of SpoIVA and ExsA/SafA were markedly decreased at 22 h compared with 13 h, while that of CotE remained almost unchanged (Table 4). These results might reflect the temporality of coat assembly to a certain extent.

Some germinant receptor proteins (GRPs), such as GerA and GerB, localize in the inner membrane, while others, such as GerP, are located in the coat.[41,42] The CT-43 chromosome contains at least 38 GRPs belonging to different families. As revealed by RNA-seq, only *gerD* mRNA could be detected throughout the life cycle, and three genes (CH2239, CH4520, and CH4750) were expressed only at 22 h. The mRNA transcripts of the other 34 genes were all detected only starting at 13 h (Supplementary Table S4 and Figure S5 in the Supporting Information). Unfortunately, only four GRPs were identified by iTRAQ. Despite this, GerD, GerE, GerM, and GerPC were up-regulated by 7.3-, 1.3-, 7.1-, and 2.3-fold at 13 h compared with 9 h, respectively. Moreover, GerE and GerPC were up-regulated by 30.9- and 2.2-fold at 22 h compared with 13 h, respectively (Supplementary Table S4 in the Supporting Information). In addition, the cortex-lytic enzyme CwlJ and its partner protein GerQ as well as the cortex-lytic enzyme YaaH are located in the coat.[43,44] (Table 4).

Recently, spore maturation was found to be necessary for acquisition of full spore resistance.[45] Among the 35 spore coat and exosporium-associated proteins identified by iTRAQ, the abundances of most proteins were markedly increased at 22 h compared with 13 h. In addition, the mRNA of a spore appendage protein (CH2337) was only detected at 22 h at very high levels, and its protein abundance was increased by about 34.4-fold at 22 h compared with 13 h. Furthermore, two types of irreversible covalent cross-links, *o*,*o*′-dityrosine bond and ε-(γ-glutamyl)-lysil isopeptide bond, have been detected in coat proteins.[33] A coat-specific transglutaminase, Tgl, catalyzes the formation of an ε-(γ-glutamyl) lysine isopeptide bond to cross-link and polymerize coat proteins.[33,45,46] This transglutaminase-mediated cross-linking is believed to play an important role in coat protein assembly in the genus *Bacillus*.[47,48] In our RNA-seq data, the *tgl* gene (CH3969) encoding transglutaminase was specifically expressed at 22 h. Taken together, changes not only in the kinds of coat proteins but also (and particularly) in coat structure likely accompany the process of spore maturation.[45]

dx.doi.org/10.1021/pr4003728 | J. Proteome Res. 2013, 12, 5487−5501

Table 3. Transcriptional Profiles of the Spore Coat and Exosporium Structure- and Assemble-Associated Genes in *B. thuringiensis* CT-43

		RPKM						RPKM			
gene	gene code	7 h	9 h	13 h	22 h	gene	gene code	7 h	9 h	13 h	22 h
Spore Coat-Associated Genes											
cotA	CH4802	0	0	2466	16	*yabG*	CH0037	0	111	53	10
cotD	CH1484	0	0	159	5424	*ybaQ*	CH1157	0	0	1758	0
cotE	CH3713	0	0	11368	451	*yckK*	CH0824	88	178	556	0
cotH	CH1987	0	0	147	87242	*ycsK*	CH4131	11	16	194	1444
cotI	CH1996	0	0	5193	0	*ydhD*	CH3361	0	0	35	5
cotJA	CH0777	0	0	2059	0	*yhaX*	CH0840	0	0	4278	0
cotJB	CH0776	0	0	1311	0	*yhbA*	CH0467	8	11	15	0
cotJC	CH0775	0	0	2309	0	*yheD*	CH0829	0	0	964	0
cotM	CH3567	0	0	134	3498	*yhjR*	CH3076	0	0	21	16
cotN	CH1209	33	314	58	0	*yirY*	CH2259	39	50	13	0
cotQ	CH0356	0	0	0	292	*yisY*	CH4803	0	0	745	53
cotS	CH5010	65	147	870	0	*yisY1*	CH2439	0	0	669	0
cotSA	CH0260	0	0	222	0	*ykuD*	CH0725	0	0	0	99
cwlJ	CH5430	0	0	13940	0	*ykvP*	CH3704	0	4	50	0
exsA/safA	CH4442	0	0	4220	9	*ylbD*	CH3937	0	0	0	132
gerQ	CH5431	0	0	13838	7	*yncD*	CH2023	0	0	75	0
oxdD	CH0973	0	5	23	0	*yodI*	CH3527	0	0	0	30864
sodA	CH1396	0	0	1487	22	*ypeP*	CH1526	32	43	475	0
spoIVA	CH1436	0	0	4230	0	*yppG*	CH1483	0	0	744	42
spoVID	CH4474	0	0	5248	0	*ypzA*	CH1528	748	273	1089	0
tasA	pCT8252.6	59	163	2086	581	*ysxE*	CH4473	0	0	3005	0
tgl	CH3969	0	0	0	499	*yusA*	CH5043	366	100	14	0
yaaH	CH3554	0	0	1360	0	*yxeE*	CH3478	0	0	0	2401
						Exosporium-Associated Genes					
alr	CH0226	0	0	1680	2109	*exsC*	CH2888	0	0	0	86920
bclA	CH1144	0	0	1672	3834	*exsD*	CH2631	0	0	0	5048
bclB	CH1145	0	0	17492	17854	*exsE*	CH1663	6	6	19	3
betA	CH3416	0	0	0	787	*exsG*	CH2087	0	0	0	232
bxpB	CH1159	0	0	101	23994	*exsJ*	CH2359	0	0	151	44219
cotB1	CH0332	0	0	100	42004	*exsK*	CH2477	0	0	0	37820
cotB2	CH0333	0	0	0	11368	*exsY/cotZ*	CH1160	0	0	18571	153
cotY	CH1156	0	0	2001	6693	*inH*	CH2882	0	0	0	2100
exsA/safA	CH4442	0	0	4220	9	*sod-Mn*	CH4291	5562	9915	572	8

In our proteomics data, 10 exosporium-associated proteins were identified, and the abundances of most proteins were significantly up-regulated at 22 h compared with 13 h, including Alr (10-fold), BxpB (525-fold), CotB1(505-fold), CotB2 (52-fold), CotY (14-fold), ExsY/CotZ (3-fold), ExsK (381-fold), and InH (6-fold). The proteins BxpB, ExsY/CotZ, and CotY were confirmed to be required for exosporium assembly, and ExsA/SafA is required for both coat and exosporium assembly in the *B. cereus* group.[49−51] Whereas BclA is the major component of the exosporium hair-like nap,[52] this protein was not found in our proteomics data, and this phenomenon also appeared in another case,[53] possibly due to the unique structure of the exosporium hair-like nap.

The exosporium is a distinct glycoprotein layer with rhamnose and methyl rhamnose representing the major carbohydrate groups of the exosporium glycoprotein in *B. thuringiensis*.[54] In the *B. cereus* group genomes, the genes *bclA*, *bxpB*, *cotY*, and *exsY/cotZ* are clustered with the rhamnose biosynthesis operon (*rfbACBD*, also named as *rmlACBD*) and the genes encoding glycosyltransferases and *O*-methyltransferases.[55] Our results indicated that all genes within the CT-43 gene cluster CH1141−1160 seemed to be specifically expressed at 13 h at the mRNA level (Supplementary Table S4 and Figure S5 in the Supporting Information). Moreover, 65% (13/20) of the proteins encoded by this gene cluster were identified by iTRAQ, and the abundance of most proteins reached a peak during sporulation (Supplementary Table S4 in the Supporting Information). Consequently, the majority of genes in this gene cluster likely participate in exosporium formation.[55]

Transcriptional Regulation

Transcriptional Machineries and Their Regulatory Roles. Transcription is the first step in the process of gene expression and is carried out by RNA polymerase (RNAP). In Gram-positive bacteria like genus *Bacillus*, the RNAP core enzyme possesses five subunits ($\alpha_2\beta\beta'\omega$) and an additional subunit (δ), RpoE, is required for the specificity of RNAP. The core enzyme could interact with multiple interchangeable σ subunits (σ factor), which gives rise to multiple forms of RNAP holoenzymes. According to the features of σ factors, different forms of RNAP holoenzymes could bind to their cognate promoters to initiate transcription of specific genes (or operons).[56]

Interestingly, our RNA-seq results indicated that the gene *rpoZ* encoding the ω subunit was induced only during the stationary phase, being initiated at 9 h and up-regulated by more than two-fold at 13 h compared with 9 h (Supplementary Table S5 in the

dx.doi.org/10.1021/pr4003728 | J. Proteome Res. 2013, 12, 5487−5501

Table 4. Spore Coat and Exosporium-Associated Proteins Identified by iTRAQ

protein	7 h vs 9 h[a]	7 h vs 13 h	7 h vs 22 h	9 h vs 13 h	9 h vs 22 h	13 h vs 22 h
Alr	1.4[b]	1.5	15.0	1.0	10.0	10.0
BxpB	2331.6	6876.2	72752.3	164.5	30.6	524.8
CotA	–[c]			154.7		
CotB1	1.7	1.5	152.9	6706.4	58.5	504.7
CotB2	1.1	−1.1[d]	50.9	−1.4	37.2	51.9
CotE	5.5	24.0	13.7	8.2	6.0	−1.3
CotH				5.6	14.9	2.9
CotJB	3992.9					3.1
CotJC	1.0	6.9	20.3	7.7	19.5	2.6
CotN	1.4	1.3	3.0	1.1	2.0	2.6
CotQ						
CotY	2300.1	16.7	3566.8	3.6	20.5	13.9
CwlJ	2332.5	5338238.4	5572.5	1160.8	399.1	4.2
ExsA/SafA[e]	2.5	26.3	82.6	26.3	91.5	−4.3
ExsK	1.6	1.1	9.2	1.0	5.0	381.1
ExsY/CotZ	3103.6	9135.6	15309.1	3.6	8.6	2.8
GerQ	1.6	3.0	8.6	2.6	7.5	3.0
InH	1.6	1.5	6.0	1.0	3.3	5.9
Mn-SOD	1.0	1.1	1.1	1.1	1.1	1.0
OxdD			5.5		4.0	
SodA	1.3	3.4	6.4	2.7	5.7	2.7
SpoIVA	2299.6	3845.1	9.8	9.1	1.7	−4.2
SpoVID	2597.2	15430.5	3793.8	9.6	7.6	2.9
YaaH	1.2	4.2	13.2	3.8	11.8	3.7
YbaG	27.7	16.4	203.4	1.1	12.9	10.9
YbaQ						
YckK	−1.1	1.3	2.1	1.5	2.4	1.8
YcsK	1.1	1.4	8.9	1.4	8.8	7.6
YhaX	1.1	9.2	1.3	12.1	1.0	−3.0
YheD						
YirY	1.1	1.0	−1.1	1.0	−1.2	−1.2
YisY	31.8			3.1	7.3	3.1
YpzA	2300.6	221.3	269.9	7.0	7.3	1.1
YusA	1.0	1.4	2.4	1.4	2.3	2.0
YxeE	1.1	1.3	4.2	−1.1	5.0	3.0

[a]Protein abundance of 9 h is compared with that of 7 h; the rest may be deduced by analogy. [b]Numerical value represents the up-regulated fold change between two specific growth phases. [c]Protein abundance cannot be quantitatively compared between two specific growth phases. [d]Negative number means the down-regulated fold between two specific growth phases. [e]Same protein is assigned two different designations in two species.

Supporting Information). At the same time, iTRAQ data showed that the protein RpoZ was up-regulated by about 1.6-fold at 13 h compared with 9 h (Supplementary Table S5 in the Supporting Information). The β' subunit was observed to be more prone to proteolytic fragmentation in vitro when the RNAP of *Mycobacterium smegmatis* lacks the ω subunit.[57] In another case, the purified *Escherichia coli* RNAP lacking the ω subunit did not respond to the effector ppGpp of the stringent response in vitro.[58] The ppGpp strongly and directly inhibits the promoters for rRNA and tRNA but directly or indirectly stimulates expression of a set of genes for amino acid biosynthesis and transport.[58,59] Indeed, we found that SpoT (a bifunctional enzyme that can both synthesize and degrade ppGpp) and many proteases were markedly up-regulated during the stationary phase. Taken together, these results suggest that the increased expression of the ω subunit during the stationary phase would contribute to the prevention of the RNAP β' subunit from proteolytic fragmentation and couple to the ppGpp signaling system in transcriptional regulation of the stringent response in *B. thuringiensis*.

Another RNAP subunit deserving particular attention is the δ subunit. Because a strain containing a deletion of the *rpoE* gene is viable and shows no major alterations in gene expression, it is likely to be a dispensable subunit of RNAP in *B. subtilis*.[60,61] In the presence of δ, however, RNAP displays increased transcriptional specificity and RNA synthesis efficiency.[61,62] Moreover, inactivation of the *rpoE* gene can alleviate suppression of sporulation in *B. subtilis* at early stage III produced by disruption of the *pdhC* gene encoding the E2 subunit of pyruvate dehydrogenase, indicating that the δ subunit does have some direct or indirect role in sporulation.[60] Because the protein RpoE was up-regulated by about 1.5-fold at 13 h compared with 9 h (Supplementary Table S5 in the Supporting Information), we speculate that this increase could also have some important regulatory roles in spore and parasporal crystal formation in *B. thuringiensis*.

Except for the above-mentioned ω and δ subunits, the α, β, and β' subunits of core RNAP were all maintained at equivalent expression levels during each growth phase. Furthermore, expression of the genes *greA* (transcriptional elongation factor) and *rho* (transcriptional termination factor) were both up-regulated by about three-fold at the mRNA level at 13 h. In iTRAQ data, the abundance of GreA was increased by 1.5-fold, and Rho remained

dx.doi.org/10.1021/pr4003728 | J. Proteome Res. 2013, 12, 5487−5501

almost unchanged at 13 h. In addition, two genes (*nusB* and *nusG*) and their encoding proteins (the transcription antitermination proteins) remained almost unchanged at 13 h at the mRNA and protein levels (Supplementary Table S5 in the Supporting Information), respectively. These results implied that the transcriptional machineries were running efficiently during sporulation.

Regulatory Roles of Σ-Factors and Transcriptional Factors. The σ-factors and TFs play vital roles in gene expression regulation. The CT-43 chromosome encodes 27 σ factors and more than 50 σ-factor-associated genes (such as anti-σ-factor and anti-σ-factor antagonist) and at least 312 TFs that belong to 31 superfamilies and 59 families (Supplementary Table S5 and Figure S6 in the Supporting Information). Notably, ∼80.5% (62/77) of σ factor and σ-factor-associated genes and 55.8% (174/312) of TFs were expressed at the mRNA level under our experimental conditions (Supplementary Table S5 and Figure S6 in the Supporting Information).

We observed that the TF regulatory network were quite active during sporulation. According to the RNA-seq data: (i) the expression levels of 32 TF genes were increased and 46 TF genes were specifically induced at 13 h; (ii) the expression levels of 36 TF genes were decreased and 19 TF genes that were expressed both at 7 and 9 h were not transcribed at 13 h; (iii) eight TF genes were specifically expressed at 9 h; and (iv) 58 TF genes, which included the six specifically induced genes, were still expressed at 22 h (Supplementary Table S5 in the Supporting Information). In iTRAQ data, a total of 79 TFs were identified: 11 TFs were up-regulated while 8 TFs were down-regulated at 13 h; 41 TFs remained almost unchanged at 13 h; and 19 TFs failed to be quantified (Supplementary Table S5 in the Supporting Information). These results suggested that a complicated TF regulatory network was involved in gene expression during sporulation.

The sporulation-specific σ-factors, SigH, SigF, SigE, SigG, and SigK, are spatially and temporally activated through a "criss-cross" mechanism[63] (Figure 1B). In RNA-seq data, with the exception of *sigH* mRNA, which was detected from the exponential growth phase, the other sporulation-specific σ-factors were detected at high levels only during the stationary growth phase (Supplementary Table S5 and Figure S6 in the Supporting Information). At the protein level, within the 77 σ-factor and σ-factor-associated genes, only seven σ-factors (including SigA, SigE, SigG, SigF, SigH, SigK, and SigL) and SpoIIAA (antisigma F factor antagonist) were identified by iTRAQ (Supplementary Table S5 and Figure S6 in the Supporting Information).

Activation of Spo0A and SigH in predivisional cells leads to asymmetric division, and these factors can be mutually promoted through a positive feed-forward loop (Figure 1B). Spo0A∼P increases transcription of the *sigH* gene by repressing transcription of the repressor *abrB* genes; activated SigH, in turn, elevates transcription of the *spo0A* gene using a SigH-dependent promoter.[64] In agreement with the feed-forward loop, the mRNA level of *spo0A* peaked during the transition phase (9 h), while those of the three *abrB* genes encoded by CT-43 were undetectable after 9 h (Supplementary Table S5 in the Supporting Information). In iTRAQ data, Spo0A was separately up-regulated by 2.3- and 2.6-fold at 9 and 13 h; SigH was the only one of the sporulation-specific σ-factors that failed to be identified. The two identified AbrB factors, CH0032 and CH1953, were down-regulated by 3.2- and 1.6-fold at 13 h, respectively.

SigF is the first sporulation-specific σ-factor activated in the forespore, and its activity is necessary for processing of pro-SigE to active SigE in the mother cell.[65] SigF and SigE regulate early compartmentalized gene expression, including the genes for engulfment. After engulfment, a second round of compartmentalized gene expression occurs, with SigG and SigK becoming active in the forespore and mother cell, respectively.[63] Similarly, SigG activation in the forespore is necessary for processing of pro-SigK to active SigK in the mother cell.[65] SigG and SigK activate transcription of genes that build the structural components of the spore, including the genes for producing and transporting DPA, synthesis of spore PG, yielding the coat proteins and coat assembly as well as the DNA-protective SASPs (Figure 1B,C).[21,66] SigE and SigK also promote transcription of ICP genes for parasporal crystal development (Figure 1A,B).[16] As revealed by iTRAQ, the abundances of SigF, SigE, and SigG were increased by about 4.4-, 4.0-, and 2.2-fold at 9 h, 1.7-, 5.4-, and 3.9-fold at 13 h, and 1.4-, 4.7-, and 6.2-fold at 22 h, respectively, whereas SigK could not be quantified. In addition, the three identified RsfA factors (forespore-specific transcriptional activator), CH3923, CH4417, and CH5425, were translationally up-regulated by about 1.3-, 1.0-, and 2299.8-fold at 9 h, 16.3-, 1.5-, and 5.8-fold at 13 h, and 2.4-, 1.5-, and 47.8-fold at 22 h, respectively (Supplementary Table S5 in the Supporting Information).

Regulatory Roles of the Pyruvate Dehydrogenase Complex E2 Subunit. The *pdhABCD* operon (CH3978−CH3975) of CT-43 encodes the pyruvate decarboxylase (E1α and E1β), dihydrolipoamide acetyltransferase (E2), and dihydrolipoamide dehydrogenase (E3) subunits of the pyruvate dehydrogenase complex, which transfers pyruvate into acetyl-CoA in the central carbohydrate metabolism pathways. In RNA-seq data, the mRNA levels of the four subunits were all decreased by about 10-fold at 13 h (Supplementary Table S5 in the Supporting Information), while iTRAQ showed that the abundances of these four subunits were all decreased at 9 h and the E1α (PdhA) and E1β (PdhB) subunits were further down-regulated at 13 and 22 h. However, the E2 (PdhC) and E3 (PdhD) subunits remained almost unchanged at 13 h and were both up-regulated by 2.1-fold at 22 h (Supplementary Table S5 in the Supporting Information).

The *B. subtilis* E2 subunit was confirmed to be involved in regulating gene expression at stage III.[67] More importantly, the E2 subunit of *B. thuringiensis* can positively regulate transcription of the *cry1* class genes by binding specifically to their promoter regions.[68] These results imply that the E2 subunit could function as a transcriptional factor independent of its enzymatic activity to regulate relative gene expression at the transcriptional level.

It is a seemingly contradictory phenomenon that E2 boosts parasporal crystal formation, which would consume a great amount of material and energy, just when nutrients are deficient. However, this unique genetically regulated phenomenon would have fundamental biological significance for the insect pathogenic bacterium *B. thuringiensis*: abundant parasporal crystals could kill the host insects more effectively, which, in turn, could provide sufficient host nutrients for other members of the bacterial population or allow germination of dormant spores.[16]

Regulatory Roles of Cold Shock Proteins. Bacterial cold shock proteins (CSPs) can function as mRNA chaperones and transcription antiterminators in response to temperature downshifts and other various stresses.[69,70] For the eight CSPs encoded by CT-43: (i) CH3483 was highly expressed at both the mRNA and protein levels and remained at similar levels during the four

different growth phases, indicating its constitutive expression and housekeeping function; (ii) CH2317 and CH2318 were specifically induced at 13 h; and (iii) CH5219 was up-regulated by more than 100-fold at 13 h at the mRNA level and up-regulated by 4- and 7.6-fold at 13 and 22 h, respectively, at the protein level (Supplementary Table S5 and Figure S6 in the Supporting Information). Consequently, these CSPs could play critical roles in transcriptional and posttranscriptional regulation during sporulation.

Translational Regulation

Translational Machineries and Their Regulatory Roles. The CT-43 chromosome encodes at least 57 ribosomal structure proteins, 43 ribosomal biogenesis- and modification-associated proteins, and 15 proteins that can directly regulate translation. In addition, the CT-43 chromosome contains 13 rRNA operons, 85 tRNA genes, 21 tRNA processing- and modification-associated genes, and 37 aminoacyl-tRNA synthetase genes. In iTRAQ data, 74.8% (160/214) of the translation-associated proteins were identified (Supplementary Table S6 and Figure S7 in the Supporting Information), which was far superior to the 28% (1756/6266) of the total proteins encoded by CT-43. These results indicate the importance of maintaining efficient activity of the translational machinery. Because ribosomal biogenesis consumes vast amounts of energy, the activity or intracellular levels of the ribosome must be tightly controlled during sporulation. However, very little is known about these regulatory mechanisms.[71]

Among the 57 genes encoding ribosomal structure proteins, 53 were down-regulated at both the mRNA and protein levels (Supplementary Table S6 and Figure S7 in the Supporting Information), suggesting that intracellular levels of ribosomes were obviously decreased during sporulation. At the mRNA level, however, the genes *rplS*, *rpmB*, and *rpmH* were up-regulated by about two- to four-fold, and the *rplI* gene remained at similar levels at 13 h. Unexpectedly, the protein RpmH was the only unidentified protein among the 57 ribosomal structural proteins (Supplementary Table S6 and Figure S7 in the Supporting Information). The *rpmB* gene encoding L28 is reported to play an important role in ribosome assembly,[72] and a single nucleotide substitution in the *rplS* gene encoding L19 causes antibiotic resistance in *Salmonella typhimurium*.[73] The function of the gene *rplI* encoding L9 would be essential for viability of *B. subtilis* because the *rplI* mutant could not be obtained.[74]

The CT-43 chromosome contains 25 RimI (ribosomal-protein-alanine acetyltransferase) and six RimL (ribosomal-protein-serine acetyltransferase) homologues that catalyze acetylation of the N-terminal alanine and serine of ribosomal proteins, respectively.[75,76] At the mRNA level, three *rimI* and two *rimL* homologues were specifically induced or up-regulated at 13 h; five *rimI* and one *rimL* homologues reached their highest expression levels at 9 h (Supplementary Table S6 in the Supporting Information). CH1972 (a *rimL* gene) was the only one that was up-regulated at both the mRNA and protein levels at 13 h. Within the nine rRNA processing- and modification-associated genes encoded by CT-43, the genes *rimM*, *rlmCD*, *rluB*, and *rsuA* were up-regulated by about two- to nine-fold at 13 h at the mRNA level. At the protein level, the abundances of RimM and RluB were slightly increased at 13 h, while RsuA seemed to be expressed only at 13 h (Supplementary Table S6 in the Supporting Information). The protein RimM is associated with the maturation of the 30S ribosomal subunit.[77] The enzyme RlmCD catalyzes 5-methyl uridine (m^5U) formation in 23S rRNAs.[78] The proteins RluB and RsuA separately catalyze pseudouridylation of 23S and 16S rRNA, which promotes peptide release for translation termination.[79] In RNA-seq data, 5 (*truA2*, *truA3*, *miaA*, *truB*, and *trmE*) out of 21 tRNA processing and modification-associated genes were up-regulated, and 6 genes (four copies of *gidA*, tRNA CCA-pyrophosphorylase, and *truA*) remained almost unchanged at 13 h. In iTRAQ data, 16 tRNA processing- and modification-associated proteins were identified; among them, TrmE (tRNA modification GTPase) was up-regulated by nearly two-fold at 22 h. Consequently, these results imply that the ribosomal structural proteins, rRNA, and tRNA would be specifically and differentially processed and modified during sporulation.

The aminoacyl-tRNA synthetases (including GatA/B/C, HisS1, IleS, LysS_1, Fmt, PheS, and TrpS) for eight types of aminoacyl-tRNA were up-regulated, and mRNA levels of aminoacyl-tRNA synthetases (including AlaS, ArgS1, CysS, LysS, MetS, and ProS2) for six kinds of aminoacyl-tRNA remained at similar expression levels at 13 h. At the protein level, the aminoacyl-tRNA synthetases for 20 common amino acids were all identified, and an overwhelming majority of aminoacyl-tRNA synthetases remained almost unchanged at 13 h, except that one (CH3896) of the two isoenzymes of isoleucyl-tRNA synthetase was down-regulated by more than 1.5-fold (Supplementary Table S6 in the Supporting Information).

Furthermore, the genes for ribosome recycling (*frr*), translation initiation (*infA*, *infB*, and *infC*), elongation (*fusA*, *efp*, *tsf*, and *tuf*), termination (*prfA* and *prfB*), and recycling tRNA molecules from peptidyl-tRNA (*spoVC*) were down-regulated by two- to seven-fold at the mRNA level, but they all remained almost unchanged at the protein level during sporulation (Supplementary Table S6 in the Supporting Information). Cooperatively, the two translational repressor genes *L-psp* and *yfiA*[80,81] were separately down-regulated by about 3-fold and 55-fold at 13 h at the mRNA level, and the protein abundance of YfiA was decreased by about 1.6-fold at 13 h and 4.7-fold at 22 h, respectively.

Taking the above results together, we speculate that the differences in processing and modification of ribosomal proteins, rRNA, and tRNA (combined with the derepression of translational inhibition) could boost the rate of ribosome recycling and assembly as well as translation initiation, elongation, and termination efficiency to compensate for the reduction in ribosomal levels. These changes could provide strong guarantees for sporulation and high-level ICP production in *B. thuringiensis*.

Protein Sorting and Quality-Controlling Systems. A highly efficient and robust protein quality controlling system is required for the protein synthesis process to accomplish the proper protein folding and ensure their normal biological functions. Two main strategies, namely, molecular chaperones and general proteolysis, are employed to cope with protein folding stress in bacteria.[82,83] Expression levels of some genes in the important chaperone-protease systems of CT-43, including Tig (trigger factor), GroEL/ES, DnaK/DnaJ/GrpE, ClpC/X/P, HslV/U (also named as ClpY/Q), LonB (ATP-dependent protease), HflB (a membrane-anchored protease), and ClpB (ClpP-independent disaggregase, not encoded by *B. subtilis*),[82,83] remained high during sporulation, as revealed by both RNA-seq and iTRAQ (Supplementary Table S6 and Figure S8 in the Supporting Information). Moreover, an increase in protein levels was observed for the proteins HslU and HslV (more than three-fold), GroEL and GroES (about three-fold), McsB and ClpC (nearly two-fold), and DnaK (1.6-fold) at 13 h. Additionally,

dx.doi.org/10.1021/pr4003728 | J. Proteome Res. 2013, 12, 5487−5501

a small heat shock protein (CH2168) was specifically induced during the stationary growth phase and up-regulated by about five-fold at 13 h compared with 9 h, as revealed by iTRAQ.

In *B. subtilis*, most exported proteins are synthesized as preproteins with N-terminal signal peptides: some of these proteins are secreted directly into the growth medium, while others that are involved in cell-wall turnover, substrate binding, or the folding and modification of translocated secretory proteins need to be retained at the membrane/cell wall interface or bind with the cell wall to fulfill their function.[84,85] The largest number of proteins was predicted to be transported through the major secretory (Sec) pathway. Besides, only a small amount of exported proteins can be secreted through special-purpose pathways such as the twin-arginine translocation (Tat) pathway, the pseudopilin export pathway for competence development, and the ATP-binding cassette (ABC) transporter pathway.[84] The chromosome of CT-43 encodes four type-I signal peptidase (SPase) genes: *sipS*, *sipT*, *sipU*, and *sipW*. Type I SPases can cleave both the twin-arginine and secretory signal peptides.[86] At the transcriptional level, the house-keeping *sipS* and *sipT* genes remained almost unchanged, while *sipU* and *sipW* genes were down-regulated at 13 h. SipS and SipU were identified by iTRAQ, whereby SipS remained unchanged, while SipU was down-regulated by ~2.5-fold at the translational level (Supplementary Table S6 and Figure S8 in the Supporting Information). The SPases encoding genes *comC* (for pseudopilin-like signal peptides) and *lspA* (for lipoprotein signal peptides) were detected only at the mRNA levels: *comC* remained unchanged while *lspA* reached the highest transcriptional level at 9 h. Regarding the translocation machinery, the expression of the genes *ffh* (for signal recognition particle protein), *ftsY* (for cell division protein FtsY), *csaA* (for protein secretion chaperonin CsaA), *secA2* (for preprotein translocase subunit SecA), *secY* (for preprotein translocase subunit SecY), *secE* (for preprotein translocase subunit SecE), *secG* (for preprotein translocase subunit SecG), *secDF* (for bifunctional preprotein translocase subunit SecD/SecF), *yajC* (for preprotein translocase subunit YajC), *tatA*, and *tatC* was detected at the mRNA levels, and the expression remained high for most of them during sporulation.

Taken together, these data indicate that these chaperone-protease and protein sorting systems could be sufficient for controlling protein quality during sporulation.

CONCLUSIONS

The high-throughput transcriptomics and proteomics analyses of *B. thuringiensis* strain CT-43 allowed us to comprehensively investigate the gene expression profiles and regulatory mechanisms associated with spore and parasporal crystal formation. Our results demonstrated that during sporulation ICP genes encoded by CT-43 were specifically expressed; moreover, most of the spore structure-, assembly-, and maturation-associated genes were specifically expressed or significantly up-regulated. These findings suggest that the expression of corresponding genes displayed significant characteristics of temporality.

In transcriptional regulation, sigma factors and transcriptional factors constitute a complicated regulatory network that could be the central player. At the same time, the RNAP complex δ and ω subunits, CSPs, and the E2 subunit of the pyruvate dehydrogenase complex could cooperatively contribute to this regulatory machinery. Regarding the translation process, a high proportion of the translation-associated proteins (74.8% vs 28% of the total proteins encoded by CT-43) were identified in our iTRAQ data, underscoring the importance of maintaining efficient activity of the translational machinery. Among the 57 genes encoding ribosomal structure proteins, 53 were down-regulated at both the mRNA and protein levels, suggesting that intracellular levels of ribosomes were obviously decreased during sporulation. According to the expression feature of corresponding genes, we speculated that the differences in processing and modification of ribosomal proteins, rRNA, and tRNA combined with derepression of translational inhibition could boost the rate of ribosome recycling and assembly as well as translation initiation, elongation and termination efficiency, thereby compensating for the reduction in ribosomal levels. The efficient operation of translational machineries and powerful protein sorting and quality controlling systems would thus ensure the biosyntheses of a large quantity of proteins with normal biological functions during sporulation.

ASSOCIATED CONTENT

Supporting Information

Supplementary tables, supplementary methods, and supplementary figures. This material is available free of charge via the Internet at http://pubs.acs.org.

AUTHOR INFORMATION

Corresponding Author

*Tel/Fax: +86-27-8728-0670. E-mail: hejin@mail.hzau.edu.cn.

Author Contributions

†J.W. and H.M. contributed equally to this work.

Notes

The authors declare no competing financial interest.

ACKNOWLEDGMENTS

We thank Chinese National Human Genome Center at Shanghai (Shanghai, China) and BGI-Shenzhen (Shenzhen, China) for the technical support for the RNA-seq and iTRAQ-LC−MS/MS analyses, respectively. This work was supported by the National Natural Science Foundation of China (grants 30930004, 31070065, and 31270105), the National Basic Research Program of China (973 Program, grant 2010CB126105), and the National High-tech R&D Program of China (grant 2011AA10A205).

ABBREVIATIONS

BLAST, basic local alignment search tool; cDNA, complementary DNA; CSPs, cold shock proteins; DHDPA, dihydrodipicolinic acid; DPA, dipicolinic acid; FDR, false discovery rate; GRPs, germinant receptor proteins; ICPs, insecticidal crystal proteins; iTRAQ, isobaric tags for relative and absolute quantitation; LC-MS/MS, liquid chromatography−mass spectrometry/mass spectrometry; MW, molecular weight; NAG, N-acetyl glucosamine; NAM, N-acetyl muramic acid; ORFs, open reading frames; PBPs, penicillin-binding proteins; PG, peptidoglycan; RNAP, RNA polymerase; RNA-seq, RNA (cDNA) high throughout sequencing; RPKM, reads per kilobase per million mapped reads; SASPs, α/β-type small, acid-soluble spore proteins; TFs, transcriptional factors

REFERENCES

(1) Agaisse, H.; Lereclus, D. How does *Bacillus thuringiensis* produce so much insecticidal crystal protein? *J. Bacteriol.* **1995**, *177* (21), 6027−6032.

(2) Schnepf, E.; Crickmore, N.; Van Rie, J.; Lereclus, D.; Baum, J.; Feitelson, J.; Zeigler, D. R.; Dean, D. H. *Bacillus thuringiensis* and its

pesticidal crystal proteins. *Microbiol. Mol. Biol. Rev.* **1998**, *62* (3), 775–806.
(3) van Frankenhuyzen, K. Insecticidal activity of *Bacillus thuringiensis* crystal proteins. *J. Invertebr. Pathol.* **2009**, *101* (1), 1–16.
(4) Sanahuja, G.; Banakar, R.; Twyman, R. M.; Capell, T.; Christou, P. *Bacillus thuringiensis*: a century of research, development and commercial applications. *Plant Biotechnol. J.* **2011**, *9* (3), 283–300.
(5) He, J.; Wang, J. P.; Yin, W.; Shao, X. H.; Zheng, H. J.; Li, M. S.; Zhao, Y. W.; Sun, M.; Wang, S. Y.; Yu, Z. N. Complete genome sequence of *Bacillus thuringiensis* subsp. *chinensis* strain CT-43. *J. Bacteriol.* **2011**, *193* (13), 3407–3408.
(6) Kunst, F.; Ogasawara, N.; Moszer, I.; Albertini, A. M.; Alloni, G.; Azevedo, V.; Bertero, M. G.; Bessieres, P.; Bolotin, A.; Borchert, S.; Borriss, R.; Boursier, L.; Brans, A.; Braun, M.; Brignell, S. C.; Bron, S.; Brouillet, S.; Bruschi, C. V.; Caldwell, B.; Capuano, V.; Carter, N. M.; Choi, S. K.; Codani, J. J.; Connerton, I. F.; Danchin, A.; et al. The complete genome sequence of the gram-positive bacterium *Bacillus subtilis*. *Nature* **1997**, *390* (6657), 249–256.
(7) de Been, M.; Francke, C.; Moezelaar, R.; Abee, T.; Siezen, R. J. Comparative analysis of two-component signal transduction systems of *Bacillus cereus*, *Bacillus thuringiensis* and *Bacillus anthracis*. *Microbiology* **2006**, *152* (Pt 10), 3035–3048.
(8) Moreno-Campuzano, S.; Janga, S. C.; Pérez-Rueda, E. Identification and analysis of DNA-binding transcription factors in *Bacillus subtilis* and other Firmicutes–a genomic approach. *BMC Genomics* **2006**, *7*, 147.
(9) Wang, J. P.; Mei, H.; Zheng, C.; Qian, H. L.; Cui, C.; Fu, Y.; Su, J. M.; Liu, Z. D.; Yu, Z. N.; He, J. The metabolic regulation of sporulation and parasporal crystal formation in *Bacillus thuringiensis* revealed by transcriptomics and proteomics. *Mol. Cell. Proteomics* **2013**, *12* (5), 1363–1376.
(10) Sharma, C. M.; Hoffmann, S.; Darfeuille, F.; Reignier, J.; Findeiss, S.; Sittka, A.; Chabas, S.; Reiche, K.; Hackermüller, J.; Reinhardt, R.; Stadler, P. F.; Vogel, J. The primary transcriptome of the major human pathogen *Helicobacter pylori*. *Nature* **2010**, *464* (7286), 250–255.
(11) Yoder-Himes, D. R.; Chain, P. S.; Zhu, Y.; Wurtzel, O.; Rubin, E. M.; Tiedje, J. M.; Sorek, R. Mapping the *Burkholderia cenocepacia* niche response via high-throughput sequencing. *Proc. Natl. Acad. Sci. U.S.A.* **2009**, *106* (10), 3976–3981.
(12) Wang, L.; Feng, Z.; Wang, X.; Wang, X.; Zhang, X. DEGseq: an R package for identifying differentially expressed genes from RNA-seq data. *Bioinformatics* **2010**, *26* (1), 136–138.
(13) Liu, J.; Chen, L.; Wang, J.; Qiao, J.; Zhang, W. Proteomic analysis reveals resistance mechanism against biofuel hexane in *Synechocystis* sp. PCC 6803. *Biotechnol. Biofuels* **2012**, *5* (1), 68.
(14) Marzinke, M. A.; Choi, C. H.; Chen, L.; Shih, I. M.; Chan, D. W.; Zhang, H. Proteomic analysis of temporally stimulated ovarian cancer cells for biomarker discovery. *Mol. Cell. Proteomics* **2013**, *12* (2), 356–368.
(15) Bechtel, D. B.; Bulla, L. A., Jr. Electron microscope study of sporulation and parasporal crystal formation in *Bacillus thuringiensis*. *J. Bacteriol.* **1976**, *127* (3), 1472–1481.
(16) Bechtel, D. B.; Bulla, L. A., Jr. Ultrastructural analysis of membrane development during *Bacillus thuringiensis* sporulation. *J. Ultrastruct. Res.* **1982**, *79* (2), 121–132.
(17) Ibrahim, M. A.; Griko, N.; Junker, M.; Lee, A. *Bacillus thuringiensis*: A genomics and proteomics perspective. *Bioengineered Bugs* **2010**, *1* (1), 31–50.
(18) González-Pastor, J. E. Cannibalism: a social behavior in sporulating *Bacillus subtilis*. *FEMS Microbiol. Rev.* **2011**, *35* (3), 415–424.
(19) Hernández-Soto, A.; Del Rincón-Castro, M. C.; Espinoza, A. M.; Ibarra, J. E. Parasporal body formation via overexpression of the Cry10Aa toxin of *Bacillus thuringiensis* subsp. *israelensis*, and Cry10Aa-Cyt1Aa synergism. *Appl. Environ. Microbiol.* **2009**, *75* (14), 4661–4667.
(20) Park, H. W.; Bideshi, D. K.; Federici, B. A. Molecular genetic manipulation of truncated Cry1C protein synthesis in *Bacillus thuringiensis* to improve stability and yield. *Appl. Environ. Microbiol.* **2000**, *66* (10), 4449–4455.
(21) Paredes-Sabja, D.; Setlow, P.; Sarker, M. R. Germination of spores of *Bacillales* and *Clostridiales* species: mechanisms and proteins involved. *Trends Microbiol.* **2011**, *19* (2), 85–94.
(22) Setlow, P. Spores of *Bacillus subtilis*: their resistance to and killing by radiation, heat and chemicals. *J. Appl. Microbiol.* **2006**, *101* (3), 514–525.
(23) Magge, A.; Granger, A. C.; Wahome, P. G.; Setlow, B.; Vepachedu, V. R.; Loshon, C. A.; Peng, L.; Chen, D.; Li, Y. Q.; Setlow, P. Role of dipicolinic acid in the germination, stability, and viability of spores of *Bacillus subtilis*. *J. Bacteriol.* **2008**, *190* (14), 4798–4807.
(24) Boughton, B. A.; Dobson, R. C.; Gerrard, J. A.; Hutton, C. A. Conformationally constrained diketopimelic acid analogues as inhibitors of dihydrodipicolinate synthase. *Bioorg. Med. Chem. Lett.* **2008**, *18* (2), 460–463.
(25) Daniel, R. A.; Errington, J. Cloning, DNA sequence, functional analysis and transcriptional regulation of the genes encoding dipicolinic acid synthetase required for sporulation in *Bacillus subtilis*. *J. Mol. Biol.* **1993**, *232* (2), 468–483.
(26) Li, Y.; Davis, A.; Korza, G.; Zhang, P.; Li, Y. Q.; Setlow, B.; Setlow, P.; Hao, B. Role of a SpoVA protein in dipicolinic acid uptake into developing spores of *Bacillus subtilis*. *J. Bacteriol.* **2012**, *194* (8), 1875–1884.
(27) Vasudevan, P.; Weaver, A.; Reichert, E. D.; Linnstaedt, S. D.; Popham, D. L. Spore cortex formation in *Bacillus subtilis* is regulated by accumulation of peptidoglycan precursors under the control of sigma K. *Mol. Microbiol.* **2007**, *65* (6), 1582–1594.
(28) Popham, D. L. Specialized peptidoglycan of the bacterial endospore: the inner wall of the lockbox. *Cell. Mol. Life Sci.* **2002**, *59* (3), 426–433.
(29) Vasudevan, P.; McElligott, J.; Attkisson, C.; Betteken, M.; Popham, D. L. Homologues of the *Bacillus subtilis* SpoVB protein are involved in cell wall metabolism. *J. Bacteriol.* **2009**, *191* (19), 6012–6019.
(30) Gilmore, M. E.; Bandyopadhyay, D.; Dean, A. M.; Linnstaedt, S. D.; Popham, D. L. Production of muramic delta-lactam in *Bacillus subtilis* spore peptidoglycan. *J. Bacteriol.* **2004**, *186* (1), 80–89.
(31) Popham, D. L.; Helin, J.; Costello, C. E.; Setlow, P. Muramic lactamin peptidoglycan of *Bacillus subtilis* spores is required for spore outgrowth but not for spore dehydration or heat resistance. *Proc. Natl. Acad. Sci. U.S.A.* **1996**, *93* (26), 15405–15410.
(32) McKenney, P. T.; Driks, A.; Eskandarian, H. A.; Grabowski, P.; Guberman, J.; Wang, K. H.; Gitai, Z.; Eichenberger, P. A distance-weighted interaction map reveals a previously uncharacterized layer of the *Bacillus subtilis* spore coat. *Curr. Biol.* **2010**, *20* (10), 934–938.
(33) McKenney, P. T.; Driks, A.; Eichenberger, P. The *Bacillus subtilis* endospore: assembly and functions of the multilayered coat. *Nat. Rev. Microbiol.* **2012**, *11* (1), 33–44.
(34) Henriques, A. O; Charles, P. M., Jr. Structure, assembly, and function of the spore surface layers. *Annu. Rev. Microbiol.* **2007**, *61*, 555–588.
(35) McKenney, P. T.; Eichenberger, P. Dynamics of spore coat morphogenesis in *Bacillus subtilis*. *Mol. Microbiol.* **2012**, *83* (2), 245–260.
(36) Bergman, N. H.; Anderson, E. C.; Swenson, E. E.; Niemeyer, M. M.; Miyoshi, A. D.; Hanna, P. C. Transcriptional profiling of the *Bacillus anthracis* life cycle in vitro and an implied model for regulation of spore formation. *J. Bacteriol.* **2006**, *188*, 6092–6100.
(37) Fournier, M. L.; Paulson, A.; Pavelka, N.; Mosley, A. L.; Gaudenz, K.; Bradford, W. D.; Glynn, E.; Li, H.; Sardiu, M. E.; Fleharty, B.; Seidel, C.; Florens, L.; Washburn, M. P. Delayed correlation of mRNA and protein expression in rapamycin-treated cells and a role for Ggc1 in cellular sensitivity to rapamycin. *Mol. Cell. Proteomics* **2010**, *9* (2), 271–284.
(38) Gedeon, T.; Bokes, P. Delayed protein synthesis reduces the correlation between mRNA and protein fluctuations. *Biophys. J.* **2012**, *103* (3), 377–385.
(39) Griffin, T. J.; Gygi, S. P.; Ideker, T.; Rist, B.; Eng, J.; Hood, L.; Aebersold, R. Complementary profiling of gene expression at the

transcriptome and proteome levels in *Saccharomyces cerevisiae*. *Mol. Cell. Proteomics* **2002**, *1* (4), 323−333.
(40) Lai, E. M.; Phadke, N. D.; Kachman, M. T.; Giorno, R.; Vazquez, S.; Vazquez, J. A.; Maddock, J. R.; Driks, A. Proteomic analysis of the spore coats of *Bacillus subtilis* and *Bacillus anthracis*. *J. Bacteriol.* **2003**, *185* (4), 1443−1454.
(41) Hudson, K. D.; Corfe, B. M.; Kemp, E. H.; Feavers, I. M.; Coote, P. J.; Moir, A. Localization of GerAA and GerAC germination proteins in the *Bacillus subtilis* spore. *J. Bacteriol.* **2001**, *183* (14), 4317−4322.
(42) Paidhungat, M.; Setlow, P. Localization of a germinant receptor protein (GerBA) to the inner membrane of *Bacillus subtilis* spores. *J. Bacteriol.* **2001**, *183* (13), 3982−3990.
(43) Chirakkal, H.; O'Rourke, M.; Atrih, A.; Foster, S. J.; Moir, A. Analysis of spore cortex lytic enzymes and related proteins in *Bacillus subtsilis* endospore germination. *Microbiology* **2002**, *148* (Pt 8), 2383−2392.
(44) Heffron, J. D.; Lambert, E. A.; Sherry, N.; Popham, D. L. Contributions of four cortex lytic enzymes to germination of *Bacillus anthracis* spores. *J. Bacteriol.* **2010**, *192* (3), 763−770.
(45) Sanchez-Salas, J. L.; Setlow, B.; Zhang, P. F.; Li, Y. Q.; Setlow, P. Maturation of released spores is necessary for acquisition of full spore heat resistance during *Bacillus subtilis* sporulation. *Appl. Environ. Microbiol.* **2011**, *77* (19), 6746−6754.
(46) Kobayashi, K.; Kumazawa, Y.; Miwa, K.; Yamanaka, S. ε-(γ-Glutamyl)lysine cross-links of spore coat proteins and transglutaminase activity in *Bacillus subtilis*. *FEMS Microbiol. Lett.* **1996**, *144* (2−3), 157−160.
(47) Monroe, A.; Setlow, P. Localization of the transglutaminase cross-linking sites in the *Bacillus subtilis* spore coat protein GerQ. *J. Bacteriol.* **2006**, *188* (21), 7609−7616.
(48) Zilhao, R.; Isticato, R.; Martins, L. O.; Steil, L.; Volker, U.; Ricca, E.; Moran, C. P., Jr.; Henriques, A. O. Assembly and function of a spore coat-associated transglutaminase of *Bacillus subtilis*. *J. Bacteriol.* **2005**, *187* (22), 7753−7764.
(49) Bailey-Smith, K.; Todd, S. J.; Southworth, T. W.; Proctor, J.; Moir, A. The ExsA protein of *Bacillus cereus* is required for assembly of coat and exosporium onto the spore surface. *J. Bacteriol.* **2005**, *187* (11), 3800−3806.
(50) Johnson, M. J.; Todd, S. J.; Ball, D. A.; Shepherd, A. M.; Sylvestre, P.; Moir, A. ExsY and CotY are required for the correct assembly of the exosporium and spore coat of *Bacillus cereus*. *J. Bacteriol.* **2006**, *188* (22), 7905−7913.
(51) Thompson, B. M.; Hsieh, H. Y.; Spreng, K. A.; Stewart, G. C. The co-dependency of BxpB/ExsFA and BclA for proper incorporation into the exosporium of *Bacillus anthracis*. *Mol. Microbiol.* **2011**, *79* (3), 799−813.
(52) Sylvestre, P.; Couture-Tosi, E.; Mock, M. A collagen-like surface glycoprotein is a structural component of the *Bacillus anthracis* exosporium. *Mol. Microbiol.* **2002**, *45* (1), 169−178.
(53) Redmond, C.; Baillie, L. W.; Hibbs, S.; Moir, A. J.; Moir, A. Identification of proteins in the exosporium of *Bacillus anthracis*. *Microbiology* **2004**, *150* (Pt 2), 355−363.
(54) Garcia-Patrone, M.; Tandecarz, J. S. A glycoprotein multimer from *Bacillus thuringiensis* sporangia: dissociation into subunits and sugar composition. *Mol. Cell. Biochem.* **1995**, *145* (1), 29−37.
(55) Todd, S. J.; Moir, A. J.; Johnson, M. J.; Moir, A. Genes of *Bacillus cereus* and *Bacillus anthracis* encoding proteins of the exosporium. *J. Bacteriol.* **2003**, *185* (11), 3373−3378.
(56) Haugen, S. P.; Ross, W.; Gourse, R. L. Advances in bacterial promoter recognition and its control by factors that do not bind DNA. *Nat. Rev. Microbiol.* **2008**, *6* (7), 507−519.
(57) Mathew, R.; Ramakanth, M.; Chatterji, D. Deletion of the gene *rpoZ*, encoding the omega subunit of RNA polymerase, in *Mycobacterium smegmatis* results in fragmentation of the beta' subunit in the enzyme assembly. *J. Bacteriol.* **2005**, *187* (18), 6565−6570.
(58) Vrentas, C. E.; Gaal, T.; Ross, W.; Ebright, R. H.; Gourse, R. L. Response of RNA polymerase to ppGpp: requirement for the omega subunit and relief of this requirement by DksA. *Genes Dev.* **2005**, *19* (19), 2378−2387.
(59) Paul, B. J.; Barker, M. M.; Ross, W.; Schneider, D. A.; Webb, C.; Foster, J. W.; Gourse, R. L. DksA: A critical component of the transcription initiation machinery that potentiates the regulation of rRNA promoters by ppGpp and the initiating NTP. *Cell* **2004**, *118* (3), 311−322.
(60) Gao, H.; Aronson, A. I. The delta subunit of RNA polymerase functions in sporulation. *Curr. Microbiol.* **2004**, *48* (6), 401−404.
(61) López de Saro, F. J.; Yoshikawa, N.; Helmann, J. D. Expression, abundance, and RNA polymerase binding properties of the delta factor of *Bacillus subtilis*. *J. Biol. Chem.* **1999**, *274* (22), 15953−15958.
(62) Seepersaud, R.; Needham, R. H.; Kim, C. S.; Jones, A. L. Abundance of the delta subunit of RNA polymerase is linked to the virulence of *Streptococcus agalactiae*. *J. Bacteriol.* **2006**, *188* (6), 2096−2105.
(63) Higgins, D.; Dworkin, J. Recent progress in *Bacillus subtilis* sporulation. *FEMS Microbiol. Rev.* **2012**, *36* (1), 131−148.
(64) de Hoon, M. J.; Eichenberger, P.; Vitkup, D. Hierarchical evolution of the bacterial sporulation network. *Curr. Biol.* **2010**, *20* (17), R735−R745.
(65) Eichenberger, P.; Fujita, M.; Jensen, S. T.; Conlon, E. M.; Rudner, D. Z.; Wang, S. T.; Ferguson, C.; Haga, K.; Sato, T.; Liu, J. S.; Losick, R. The program of gene transcription for a single differentiating cell type during sporulation in *Bacillus subtilis*. *PLoS Biol.* **2004**, *2* (10), e328.
(66) Abee, T.; Groot, M. N.; Tempelaars, M.; Zwietering, M.; Moezelaar, R.; van der Voort, M. Germination and outgrowth of spores of *Bacillus cereus* group members: diversity and role of germinant receptors. *Food Microbiol.* **2011**, *28* (2), 199−208.
(67) Gao, H. C.; Jiang, X.; Pogliano, K.; Aronson, A. I. The E1β and E2 subunits of the *Bacillus subtilis* pyruvate dehydrogenase complex are involved in regulation of sporulation. *J. Bacteriol.* **2002**, *184* (10), 2780−2788.
(68) Walter, T.; Aronson, A. Specific binding of the E2 subunit of pyruvate dehydrogenase to the upstream region of *Bacillus thuringiensis* protoxin genes. *J. Biol. Chem.* **1999**, *274* (12), 7901−7906.
(69) Phadtare, S. Recent developments in bacterial cold-shock response. *Curr. Issues Mol. Biol.* **2004**, *6* (2), 125−136.
(70) Sachs, R.; Max, K. E.; Heinemann, U.; Balbach, J. RNA single strands bind to a conserved surface of the major cold shock protein in crystals and solution. *RNA* **2012**, *18* (1), 65−76.
(71) Nanamiya, H.; Kawamura, F. Towards an elucidation of the roles of the ribosome during different growth phases in *Bacillus subtilis*. *Biosci. Biotechnol. Biochem.* **2010**, *74* (3), 451−461.
(72) Maguire, B. A.; Wild, D. G. The effects of mutations in the *rpmB,G* operon of *Escherichia coli* on ribosome assembly and ribosomal protein synthesis. *Biochim. Biophys. Acta* **1997**, *1353* (2), 137−147.
(73) Maisnier-Patin, S.; Berg, O. G.; Liljas, L.; Andersson, D. I. Compensatory adaptation to the deleterious effect of antibiotic resistance in *Salmonella typhimurium*. *Mol. Microbiol.* **2002**, *46* (2), 355−366.
(74) Ohashi, Y.; Inaoka, T.; Kasai, K.; Ito, Y.; Okamoto, S.; Satsu, H.; Tozawa, Y.; Kawamura, F.; Ochi, K. Expression profiling of translation-associated genes in sporulating *Bacillus subtilis* and consequence of sporulation by gene inactivation. *Biosci. Biotechnol. Biochem.* **2003**, *67* (10), 2245−2253.
(75) Tanaka, S.; Matsushita, Y.; Yoshikawa, A.; Isono, K. Cloning and molecular characterization of the gene *rimL* which encodes an enzyme acetylating ribosomal protein L12 of *Escherichia coli* K12. *Mol. Gen. Genet.* **1989**, *217* (2−3), 289−293.
(76) Vetting, M. W.; Bareich, D. C.; Yu, M.; Blanchard, J. S. Crystal structure of RimI from *Salmonella typhimurium* LT2, the GNAT responsible for N(alpha)-acetylation of ribosomal protein S18. *Protein Sci.* **2008**, *17* (10), 1781−1790.
(77) Lövgren, J. M.; Bylund, G. O.; Srivastava, M. K.; Lundberg, L. A.; Persson, O. P.; Wingsle, G.; Wikström, P. M. The PRC-barrel domain of the ribosome maturation protein RimM mediates binding to ribosomal protein S19 in the 30S ribosomal subunits. *RNA* **2004**, *10* (11), 1798−1812.
(78) Desmolaize, B.; Fabret, C.; Brégeon, D.; Rose, S.; Grosjean, H.; Douthwaite, S. A single methyltransferase YefA (RlmCD) catalyses both

m^{5}U747 and m^{5}U1939 modifications in *Bacillus subtilis* 23S rRNA. *Nucleic Acids Res.* **2011**, *39* (21), 9368−9375.
(79) Ejby, M.; Sørensen, M. A.; Pedersen, S. Pseudouridylation of helix 69 of 23S rRNA is necessary for an effective translation termination. *Proc. Natl. Acad. Sci. U.S.A.* **2007**, *104* (49), 19410−19415.
(80) Agafonov, D. E.; Kolb, V. A.; Spirin, A. S. Ribosome-associated protein that inhibits translation at the aminoacyl-tRNA binding stage. *EMBO Rep.* **2001**, *2* (5), 399−402.
(81) Morishita, R.; Kawagoshi, A.; Sawasaki, T.; Madin, K.; Ogasawara, T.; Oka, T.; Endo, Y. Ribonuclease activity of rat liver perchloric acid-soluble protein, a potent inhibitor of protein synthesis. *J. Biol. Chem.* **1999**, *274* (29), 20688−20692.
(82) Frees, D.; Savijoki, K.; Varmanen, P.; Ingmer, H. Clp ATPases and ClpP proteolytic complexes regulate vital biological processes in low GC, Gram-positive bacteria. *Mol. Microbiol.* **2007**, *63* (5), 1285−1295.
(83) Molière, N.; Turgay, K. Chaperone-protease systems in regulation and protein quality control in *Bacillus subtilis*. *Res. Microbiol.* **2009**, *160* (9), 637−644.
(84) Tjalsma, H.; Antelmann, H.; Jongbloed, J. D.; Braun, P. G.; Darmon, E.; Dorenbos, R.; Dubois, J. Y.; Westers, H.; Zanen, G.; Quax, W. J.; Kuipers, O. P.; Bron, S.; Hecker, M.; van Dijl, J. M. Proteomics of protein secretion by *Bacillus subtilis*: separating the ″secrets″ of the secretome. *Microbiol. Mol. Biol. Rev.* **2004**, *68* (2), 207−233.
(85) von Heijne, G. Protein transport: Life and death of a signal peptide. *Nature* **1998**, *396* (6707), 111−113.
(86) Tjalsma, H.; Bolhuis, A.; van Roosmalen, M. L.; Wiegert, T.; Schumann, W.; Broekhuizen, C. P.; Quax, W. J.; Venema, G.; Bron, S.; van Dijl, J. M. Functional analysis of the secretory precursor processing machinery of *Bacillus subtilis*: identification of a eubacterial homolog of archaeal and eukaryotic signal peptidases. *Genes Dev.* **1998**, *12* (15), 2318−2331.